Journal of Solid State Chemistry **155,** 71–77 (2000)
doi:10.1006/jssc.2000.8893, available online at http://www.idealibrary.com on IDEAL®

Experimental Investigation in the Quaternary Systems Ti–Ni–Al–N and Ti–Ni–Al–O

B. Huneau,*,† J. J. Ding,* P. Rogl,*,[1] J. Bauer,† X. Y. Ding,‡ and M. Bohn§

*Institut für Physikalische Chemie, Universität Wien, Währingerstraße 42, A-1090 Wien, Austria; †Laboratoire de Chimie du Solide et Inorganique Moléculaire, UMR CNRS 6511, Université de Rennes I, Avenue du Général Leclerc, F-35042 Rennes Cedex, France; ‡Department of Ferrous Metallurgy, Northeastern University, Shenyang, Liaoning, 110006, People's Republic of China; and §UMR CNRS 6538, Centre de la Microsonde Electronique de l'Ouest, IFREMER, F-29263 Plouzané, France

Received June 6, 2000; in revised form July 18, 2000; accepted July 27, 2000

DEDICATED TO PROFESSOR J. M. HONIG

The experimental evaluation of phase equilibria in the Ti–Ni–Al–N and Ti–Ni–Al–O phase diagrams are based on alloy samples, which were prepared of elemental powder blends by argon-levitation melting in a *Hukin* crucible. The experimental investigation employed X-ray powder diffraction, metallography, SEM, and EMPA techniques in the as-cast state as well as after annealing at 900°C. Two quaternary compounds Ti_3NiAl_2N and Ti_3NiAl_2O deriving from the filled Ti_2Ni type (η phase) were observed. The novel phases are in equilibrium with the Ti_2Ni-type solid solution phase $(Ti_{1-x}Al_x)_2Ni$, which exhibits a maximum solubility of 14 at.% Al in binary Ti_2Ni. Atom order in all these phases was monitored by quantitative X-ray powder diffraction (Rietveld analyses). The difference of X-ray spectra among the various phases deriving from parent Ti_2Ni type was analyzed and the complex atom site occupation mode was discussed in terms of the general classification scheme for η phases.

INTRODUCTION

High-strength, heat-, and oxidation-resistant Ti–Ni–Al alloys have recently attracted widespread attention, competing with nickel-based superalloys for high-temperature applications (1). Nothing, however, is known so far about the performance of these alloys under nitrogen/oxygen or using TiN_{1-x}/TiO_{2-x} and nitride/oxide precipitates as strengtheners. The present report in continuation of our systematic studies of phase equilibria and crystal data within the quaternary Ti–Ni–Al–N and Ti–Ni–Al–O presents experimental details on the crystal structure of Ti_3NiAl_2N and some of its phase relations within Ti–Ni–Al–N. This work also covers phase equilibria in the Ti–Ni–Al–O system as well as the formation of an isotypic quaternary oxide.

EXPERIMENTAL

Nine quaternary samples in each of the Ti–Ni–Al–N and Ti–Ni–Al–O systems have been prepared by high-frequency levitation melting starting from high-purity powders (purity > 99.9 mass%) of Ti (Johnson-Matthey & Co., UK), Ni (Research Chemicals, Princeton, NJ), and Al, TiN, and TiO_2 (Alfa, Karlsruhe, Germany), which served to introduce the properly calculated amount of nitrogen/oxygen to the alloys. The well-blended powder mixtures with a total amount of about 3 g were compacted in $\varnothing = 8$ mm steel dies without the use of lubricants and were out-gassed prior to melting under Ti/Zr-gettered high-purity argon atmosphere. For better homogeneity the samples were remelted twice or thrice, and a part of each alloy was successively subjected to a long-term annealing at 900°C for 240 h in evacuated and sealed silica tubes whose internal surface was lined with Mo foil to protect the sample alloy from attack by the hot quartz walls. After heat treatment in a thermocouple controlled wire-wound tube furnace, the alloys were quenched by rapidly submerging the quartz capsules in water. Experimental details of sample preparation and for X-ray powder diffraction experiments, LOM, and quantitative microprobe measurements have in part been given in one of our foregoing manuscripts (2). Full-matrix full-profile Rietveld refinements were carried out with a PC version of the program by Rodriguez (3) on X-ray intensities that were recorded from a flat specimen in the D-5000 diffractometer or from an image-plate Guinier–Huber system.

Quantitative composition analyses for the Ti–Ni–Al–N samples were performed on as-cast and annealed alloys on a CAMEBAX SX50 wavelength dispersive spectrograph comparing the $K\alpha$ emissions of the four elements in the alloys with those from elemental standards and a VN standard and applying a deconvolution and ZAF correction procedure (4). The experimental parameters employed were acceleration voltage of 15 kV, sample current of 20 nA, and

---

[1] To whom correspondence should be addressed. E-mail: peter.franz.rogl@univie.ac.at.

0022-4596/00 $35.00

spectrometer crystals such as PET for Ti*K*α, TAP for Al*K*α, LiF for Ni*K*α, and PC1 for the N*K*α radiation. Microstructure examination of Ti–Ni–Al–O samples annealed at 900°C was performed on a Zeiss DSM 962 with a Link EDX system measuring the *K*α emissions of the metals under 25 kV and 0.57 μA sample current.

RESULTS AND DISCUSSION

a. Phase Relations in Ti–Ni–Al–N and Ti–Ni–Al–O Systems

Crystallographic data from X-ray powder diffraction and EMPA results for the systems Ti–Ni–Al–N and Ti–Ni–Al–O are summarized in Tables 1 and 2, revealing partial phase relations in the quaternary involving new type quaternary phases with composition Ti_3NiAl_2N and Ti_3NiAl_2O (Ti_2Ni-derivative type, see below). Variations of the lattice parameters and of the composition in EMPA (see Table 1) indicate a small but significant homogeneous region. The EMPA data also reveal a small deficiency in nitrogen (12.4 ± 7 at.% N in contrast to 14.3 at.% N in the ideal formula). It is important to note that in all the quaternary alloys investigated there was practically no solubility for nitrogen for the binary and ternary phases encountered from the Ti–Ni–Al system. Refining these EMPA data of the nitride phase taking oxygen as a fifth element being the difference weight to 100 mass%, we obtain 550 ppm O, which may account for some further filling of the nonmetal lattice site (see below). Figure 1 shows the microstructure of alloy $Ti_{37}Ni_{28.6}Al_{20.1}N_{14.3}$ after annealing at 900°C, revealing the quaternary phase Ti_3NiAl_2N in equilibrium with TiN and several nitrogen-free phases from the Ti–Ni–Al ternary system. The microstructures of the alloys $Ti_{28.57}Ni_{28.57}Al_{28.57}O_{14.29}$ and $Ti_{42.86}Ni_{14.28}Al_{28.57}O_{14.29}$ show the coexistence of the solid solution $(Ti,Al)_2Ni$ (expanding from binary Ti_2Ni) with the Ti_3NiAl_2O phase (see Fig. 2). Practically isotypic both these phases derive from the Ti_2Ni-parent type; however, they differ with respect to atom order and nonmetal interstitials (for structural details see below). A closer inspection of the oxygen content in the Ti_3NiAl_2O phase by quantitative EMPA revealed a composition with 13.2 ± 6 at.% O, rather close to the nominal values.

b. X-Ray Diffraction

b.1. Rietveld refinement of the crystal structures of $(Ti_{1-x}Al_x)_2Ni$, Ti_3NiAl_2N and Ti_3NiAl_2O. Table 3 summarizes the results of the Rietveld X-ray refinement of the quaternary alloys $Ti_{47}Ni_{28.6}Al_{10.14}N_{14.3}$, Ti_3NiAl_2N, and $Ti_{44.5}Ni_{14.8}Al_{29.6}N_{11.1}$ in comparison with the ternary alloy $Ti_{56.8}Ni_{29}Al_{14.2}$, which exhibits the maximum Al solubility in binary Ti_2Ni. In all these alloys the main phase crystallizes with the Ti_2Ni type with various atom site occupations. In agreement with the extension of the phase field $(Ti_{1-x}Al_x)_2Ni$ at constant Ni content aluminium atoms substitute for Ti atoms in the 48*f* position $(x, \frac{1}{8}, \frac{1}{8})$ of space group $Fd\bar{3}m$ up to 75%. It is interesting to note that titanium atoms in the 16*c* position (0,0,0) at the centers of metal icosahedra show no preference for Ti/Al exchange; Ni atoms are in the 32e sites (*x*,*x*,*x*). One may assume that nitrogen atoms, upon entering the quaternary system, will simply occupy the center positions of the octahedral voids provided by the metal host lattice. The new quaternary compound, Ti_3NiAl_2N, however, shows a completely different metal atom occupation scheme with Ti atoms in the 48*f* positions, Ni atoms in the 16*c* sites, and Al atoms in the 32*e* positions. The nitrogen atoms are localized in the 16*d* sites $(\frac{1}{2}, \frac{1}{2}, \frac{1}{2})$ with octahedral coordination $[Ti_6]N$ formed by six Ti atoms. From EMPA and the Rietveld analyses we only observe a small homogeneity range with minor Ni/Al exchange in the 32*e* and 16*c* sites (one atom per site; see Table 3). A similar occupation scheme is obtained from Rietveld analysis of the corresponding oxygen-containing alloy Ti_3NiAl_2O.

With respect to the phase equilibria listed in Tables 1 and 2, and in combination with the results of the Rietveld refinement, we thus may safely assume that neither the ternary solid solution $(Ti,Al)_2Ni$ nor the ternary phases $Ti_4Ni_2(N,O)$ show any connectivity with the quaternary compounds $Ti_3NiAl_2(N,O)$ via atom site exchange accompanied by successive nitrogen/oxygen incorporation. These results are then consistent with the formation of truly quaternary compounds Ti_3NiAl_2N and Ti_3NiAl_2O deriving from the Ti_2Ni-type parent structure.

From the viewpoint of structural chemistry the fully ordered crystal structure of Ti_3NiAl_2N corresponds to Ta_3CrAl_2C first reported by Reiffenstein *et al.* (5). The mode of site occupation and filling the octahedral voids in the so-called *η* phases deriving from the parent Ti_2Ni type was earlier extensively discussed by Rogl and Nowotny (6). Referring to this analysis $(Ti_{1-x}Al_x)_2Ni$ must be classified as a filled metal host lattice structure where the titanium atoms (in 16*c*) at the centers of the metal icosahedra (each formed by six Ti/Al) atoms in 48*f* and six Ni atoms in 32*e* do not allow for Ti/Al substitution. For *η* carbides with the stoichiometry $M_3M''M'_2C$ such as Ta_3CrAl_2C (5) or Ti_3NiAl_2C (7), however, we observe the small transition metal such as chromium or nickel at the centers of the metal icosahedra, the latter now formed by Ti (Ta) in 48*f* and Al in 32*e* positions. This occupation scheme essentially corresponds with the atom site distribution in Ti_3NiAl_2N and Ti_3NiAl_2O. Nonmetal atoms such as C, N, or O are assumed to occupy the octahedral voids in 16*d* but may also enter the octahedral voids in the 8*a* sites $(\frac{1}{8}, \frac{1}{8}, \frac{1}{8})$. Due to the rather small X-ray scattering power of the nitrogen/oxygen atoms a further precision in the distribution of these light atoms can only be awaited from neutron diffraction experiments.

TABLE 1
Crystallographic Data and EMPA Results for Quaternary Ti–Ni–Al–N Alloys

Nominal composition in at.%				Heat treatment	X-ray phase analysis	Space group	Pearson symbol	Structure type	Lattice parameters (pm)		Volume (10^6 pm^3)	Results of EMPA in at.%			
Ti	Ni	Al	N						*a*	*c*	*V*	Ti	Ni	Al	N
47	28.6	10.1	14.3	Arc	TiN	$Fm\bar{3}m$	cF8	NaCl	422.96(2)		75.665(8)				
					$(Ti_{1-x}Al_x)_2Ni$	$Fd\bar{3}m$	cF96	Ti_2Ni	1124.91(8)		1423.5(2)				
				900°C	TiN	$Fm\bar{3}m$	cF8	NaCl	422.61(2)		75.477(8)	58.9(6)	0.2(1)	0	40.9(6)
					$(Ti_{1x}Al_x)_2Ni$	$Fd\bar{3}m$	cF96	Ti_2Ni	1128.15(10)		1435.8(3)	59.3(7)	32.8(4)	7.9(5)	0
					τ_4-$TiNi_2Al$	$Fm\bar{3}m$	cF16	BiF_3				28.9(5)	48.8(4)	22.3(5)	0
					TiNi	$Pm\bar{3}m$	cP2	CsCl				47.1(3)	47.3(2)	5.6(1)	0
37	28.6	20.1	14.3	Arc	TiN	$Fm\bar{3}m$	cF8	NaCl	423.29(2)		75.845(9)				
					Ti_3NiAl_2N	$Fd\bar{3}m$	cF112	der.Ti_2Ni[a]	1137.01(4)		1469.9(1)				
				900°C	TiN	$Fm\bar{3}m$	cF8	NaCl	423.32(3)		75.86(1)	50.6(5)	0.1	—	49.3(5)
					Ti_3NiAl_2N	$Fd\bar{3}m$	cF112	der.Ti_2Ni	1137.60(6)		1472.2(1)	44.2(4)	14.8(2)	28.6(2)	12.4(7)
					τ_3-Ti_2NiAl_3	$P6_3/mmc$	hP12	$MgZn_2$				35.3(1)	25.9(2)	38.8(1)	0
					τ_4-$TiNi_2Al$	$Fm\bar{3}m$	cF16	BiF_3				25.4(1)	48.9(2)	25.7(1)	0
28.6	28.6	28.6	14.3	Arc	TiN	$Fm\bar{3}m$	cF8	NaCl	423.70(1)		76.062(4)				
				900°C	TiN	$Fm\bar{3}m$	cF8	NaCl	423.22(3)		75.80(1)	53.7(4)	0.5(1)	0.2(2)	45.6(5)
					NiAl	$Fm\bar{3}m$	cP2	CsCl	289.31(4)		24.22(1)	7.9(4)	49.0(2)	43.1(5)	0
42.9	14.3	28.6	14.3	Arc	TiN	$Fm\bar{3}m$	cF8	NaCl	423.13(6)		75.76(2)				
					Ti_3NiAl_2N	$Fd\bar{3}m$	cF112	der.Ti_2Ni	1137.02(6)		1469.9(1)				
				900°C	TiN	$Fm\bar{3}m$	cF8	NaCl	423.18(4)		75.78(1)				
					Ti_3NiAl_2N	$Fd\bar{3}m$	cF112	der.Ti_2Ni	1137.37(4)		1471.3(1)				

[a] Derivative of Ti_2Ni type.

TABLE 2
Crystallographic Data and EMPA Results for Quaternary Ti–Ni–Al–O Alloys at 900°C

Nominal composition in at.%				Heat treatment	X-ray phase analysis	Space group	Pearson symbol	Structure type	Lattice parameters (pm)		Volume (10^6 pm^3)	Results of EMPA in at.%			
Ti	Ni	Al	O						*a*	*c*	*V*	Ti	Ni	Al	O
47	28.6	10.1	14.3	Arc	$(Ti_{1-x}Al_x)_2Ni$	$Fd\bar{3}m$	cF96	Ti_2Ni	1123.48(11)		1418.1(2)				
					τ_4-$TiNi_2Al$	$Fm\bar{3}m$	cF16	BiF_3	590.83(2)		206.25(1)				
				900°C	Ti_2O	$Fm\bar{3}m$	cF8	NaCl	296.64(4)	481.71(24)	42.388(2)				
					$(Ti_{1-x}Al_x)_2Ni$	$Fd\bar{3}m$	cF96	Ti_2Ni	1124.23(12)		1420.9(1)	54.7	35.2	10.1[a]	
					τ_4-$TiNi_2Al$	$Fm\bar{3}m$	cF16	BiF_3	590.02(–)		205.41(3)	28.5	54.9	16.6[a]	
37	28.6	20.1	14.3	Arc	$(Ti_{1-x}Al_x)_2Ni$	$Fd\bar{3}m$	cF96	Ti_2Ni	1124.05(17)		1420.2(1)				
					τ_3-Ti_2NiAl_3	$P6_3/mmc$	hP12	$MgZn_2$	499.95(12)	805.10(61)	201.23(4)				
					τ_4-$TiNi_2Al$	$Fm\bar{3}m$	cF16	BiF_3	589.94(19)		205.32(1)				
				900°C	$(Ti_{1-x}Al_x)_2Ni$	$Fd\bar{3}m$	cF96	Ti_2Ni	1123.48(15)		1418.1(2)	51.5	34.2	14.1	0.2
					τ_3-Ti_2NiAl_3	$P6_3/mmc$	hP12	$MgZn_2$	500.40(11)	809.52(32)	202.71(2)	38.3	32.2	29.5	0
					τ_4-$TiNi_2Al$	$Fm\bar{3}m$	cF16	BiF_3	589.75(6)		205.12(1)	26.5	56.0	17.5	0
					Ti_3NiAl_2O	$Fd\bar{3}m$	cF112	der.Ti_2Ni	1137.71(16)		1472.6(2)	44.0	14.9	27.9	13.2
28.6	28.6	28.6	14.3	Arc	$(Ti_{1-x}Al_x)_2Ni$	$Fd\bar{3}m$	cF96	Ti_2Ni	1124.35(22)		1421.4(2)				
					τ_3-Ti_2NiAl_3	$P6_3/mmc$	hP12	$MgZn_2$	498.43(32)	802.62(18)	199.41(4)				
					τ_4-$TiNi_2Al$	$Fm\bar{3}m$	cF16	BiF_3	589.58(22)		204.94(3)				
				900°C	$(Ti_{1-x}Al_x)_2Ni$	$Fd\bar{3}m$	cF96	Ti_2Ni	1123.61(15)		1418.6(2)				
					τ_3-Ti_2NiAl_3	$P6_3/mmc$	hP12	$MgZn_2$	499.86(50)	808.99(58)	202.13(5)	53.2	20.5	26.3[a]	
					τ_4-$TiNi_2Al$	$Fm\bar{3}m$	cF16	BiF_3	589.47(14)		204.83(2)				
					Ti_3NiAl_2O	$Fd\bar{3}m$	cF112	der.Ti_2Ni	1137.91(11)		1473.4(1)				
42.9	14.3	28.6	14.3	Arc	$(Ti_{1-x}Al_x)_2Ni$	$Fd\bar{3}m$	cF96	Ti_2Ni	1130.90(–)		1446.3(1)				
					τ_3-Ti_2NiAl_3	$P6_3/mmc$	hP12	$MgZn_2$	501.73(18)	816.21(47)	205.47(2)				
					Ti_3NiAl_2O	$Fd\bar{3}m$	cF112	der.Ti_2Ni	1137.97(27)		1473.6(2)				
				900°C	$(Ti_{1-x}Al_x)_2Ni$	$Fd\bar{3}m$	cF96	Ti_2Ni	1125.24(24)		1424.7(2)	53.2	27.9	18.9[a]	
					τ_3-Ti_2NiAl_3	$P6_3/mmc$	hP12	$MgZn_2$	501.87(36)	813.19(51)	204.82(3)	37.3	30.6	32.1[a]	
					Ti_3NiAl_2O	$Fd\bar{3}m$	cF112	der.Ti_2Ni	1137.71(9)		1472.6(2)				
44.5	14.8	29.6	11.1	900°C	Ti_3NiAl_2O	$Fd\bar{3}m$	cF112	der.Ti_2Ni	1138.76(6)		1476.7(1)				
					τ_3-Ti_2NiAl_3	$P6_3/mmc$	hP12	$MgZn_2$	501.28(31)	815.19(36)	204.84(3)	53.4	19.9	26.7[a]	

[a] Oxygen not determined.

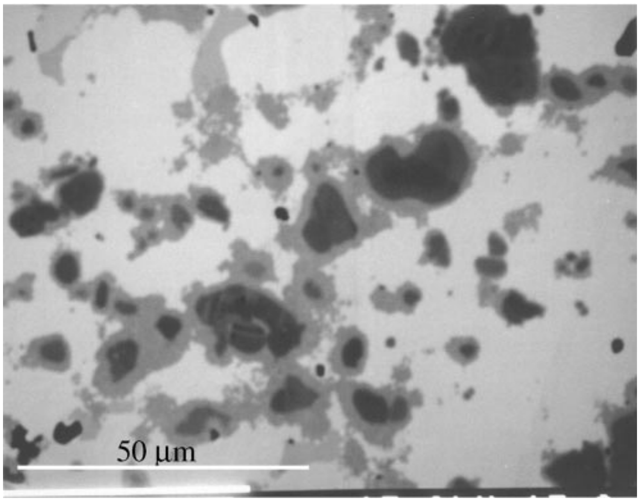

FIG. 1. Alloy $Ti_{37}Ni_{28.6}Al_{20.1}N_{14.3}$ after annealing at 900°C and quenched. BSE, image. Dark phase TiN ($Ti_{50.6}Ni_{0.1}N_{49.3}$), dark gray phase Ti_3NiAl_2N ($Ti_{44.2}Ni_{14.8}Al_{28.6}N_{12.4}$), light gray phase ($Ti_{35.3}Ni_{25.9}Al_{38.8}$), and bright phase ($Ti_{25.4}Ni_{48.9}Al_{25.7}$).

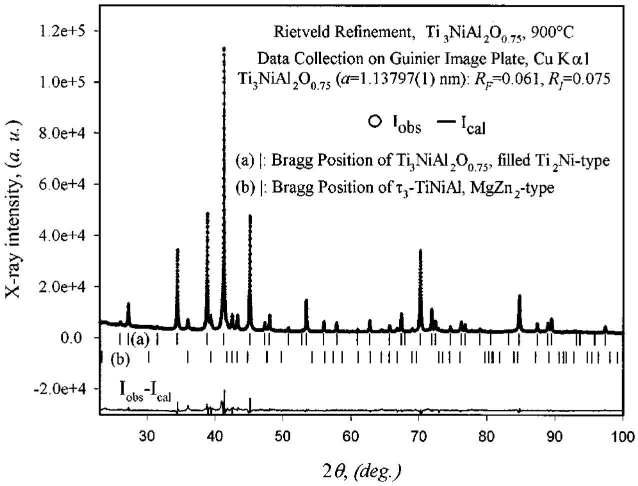

FIG. 3. Rietveld refinement of $Ti_{44.5}Ni_{14.8}Al_{29.6}O_{11.1}$ (at.%) annealed at 900°C.

b.2. On the correspondence of the x phase with $Ti_3NiAl_2O_{1-x}$. Umemoto and co-workers (8–10) reported an unknown phase with the Ti_2Ni type in the Ti–Ni–Al system. These authors suggested stabilization of this phase, labeled as x, by small amounts of oxygen. In the homologous systems Ti–{Pd, Pt}–Al–O we indeed found a quaternary oxide, $Ti_3\{Pd, Pt\}Al_2O$, deriving from the filled Ti_2Ni type (11). Speculation on isotypic behavior for the analogous Ni-containing compound and the above analysis on the Ti–Ni–Al–N alloys motivated us to investigate the Ti–Ni–Al–O system (Table 2). X-ray powder diffraction of an annealed alloy $Ti_{44.5}Ni_{14.8}Al_{29.6}O_{11.1}$ (at.%) proved a nearly single-phase oxide with a small amount of τ_3-TiNiAl ($MgZn_2$ type). The Rietveld refinement shows that the calculated diffraction pattern on the basis of the filled Ti_2Ni type and with atom order corresponding to Ti_3NiAl_2N perfectly matches the observation and thus reveals a formula $Ti_3NiAl_2O_{0.75}$ with a lattice parameter $a = 1.13797(1)$ nm (Fig. 3). The metal atoms in the quaternary oxide are completely ordered as shown in Table 3 but the site $16d$ $(\frac{1}{2}, \frac{1}{2}, \frac{1}{2})$ is not fully occupied by O atoms (only about 75%).

To reveal the characteristic differences in the X-ray intensities depending on the atom site occupation, we calculated model X-ray spectra (Fig. 4) for the various phases that crystallize with the Ti_2Ni-parent type: Ti_2Ni, Ti_4Ni_2O, $(Ti,Al)_4(Ni,Al)_2O$ with random Al distribution in Ti and Ni sites and ordered Ti_3NiAl_2O. Comparing these X-ray spectra in Fig. 4, the major features of the Ti_3NiAl_2O spectrum are easily observed: a weak X-ray intensity for the crystallographic planes (111) at $2\theta = 13.4°$ and (442) at $2\theta = 47.9°$, but, a strong intensity for the reflections (331) at

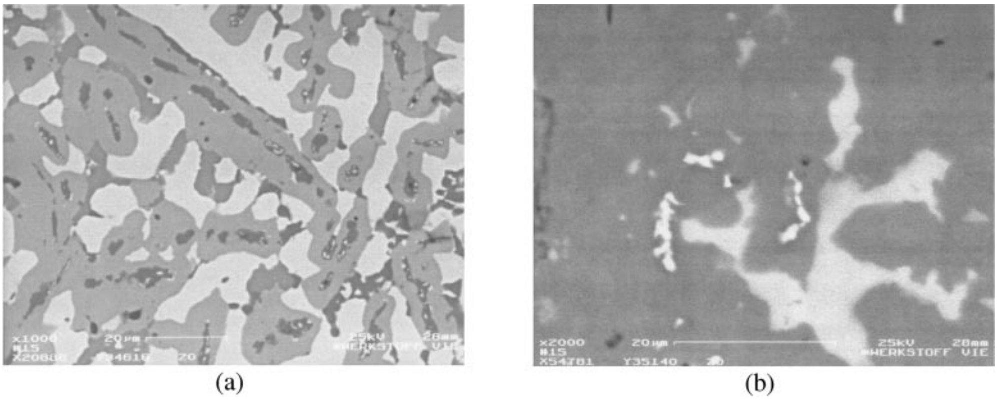

FIG. 2. Alloy (a) $Ti_{28.6}Ni_{28.6}Al_{28.6}O_{14.3}$ (white, τ_4; gray, $(Ti,Al)_2Ni$; dark gray, τ_3; dark, Ti_3NiAl_2O) and (b) $Ti_{42.9}Ni_{14.3}Al_{28.6}O_{14.3}$ (gray matrix: Ti_3NiAl_2O; white, $(Ti,Al)_2Ni$; white gray, τ_3) annealed at 900°C, primary electron image.

TABLE 3
Rietveld Refinements for $(Ti_{1-x}Al_x)_2Ni$, Ti_3NiAl_2N, and Ti_3NiAl_2O

Parameter/compound Nominal composition in at.%	$(Ti_{1-x}Al_x)_2Ni$ $Ti_{56.8}Ni_{29}Al_{14.2}$	$Ti_3(Ni,Al)_3N$ $Ti_{37}Ni_{28.6}Al_{20.1}N_{14.3}$	Ti_3NiAl_2N $Ti_{42.8}Ni_{14.3}Al_{28.6}N_{14.3}$	Ti_3NiAl_2O $Ti_{44.5}Ni_{14.8}Al_{29.6}O_{11.1}$
a (nm)	1.12316(5)	1.13684(2)	1.13685(2)	1.13797(1)
V (nm^3)	1.41687	1.46926	1.46929	1.47369
Data collection	D5000, Cu$K\alpha$	D5000, Cu$K\alpha$	D5000, Cu$K\alpha$	Image plate Cu$K\alpha_1$
2Θ range	10°–110°	10°–110°	10°–110°	8°–100°
Number of variables	25	24	24	24
$R_F = \sum\lvert F_o - F_c\rvert/\sum F_o$	0.035	0.027	0.038	0.061
$R_I = \sum\lvert I_o - I_c\rvert/\sum I_o$	0.052	0.034	0.049	0.075
$R_{wP} = [\sum w_i\lvert y_{oi} - y_{cI}\rvert^2/\sum w_i\lvert y_{oi}\rvert^2]^{1/2}$	0.139	0.128	0.166	0.067
$R_P = \sum\lvert y_{oi} - y_{ci}\rvert/\sum\lvert y_{oi}\rvert$	0.110	0.099	0.118	0.046
$R_e = \{(N - P + C)/(\sum w_i\lvert y_{oi}\rvert^2)\}^{1/2}$	0.076	0.069	0.059	0.036
$\chi^2 = (R_{wP}/R_e)^2$	3.35	3.38	8.04	17.8
Atom parameters				
M1 in $48f$ (x, 1/8, 1/8)	36Ti + 12Al	48Ti	48Ti	48Ti
x	0.4392(2)	0.4391(2)	0.4390(2)	0.4369(1)
$B_{eq}.(B_{iso})\ 10^2$ (nm^2)	1.73(8)	1.39(6)	2.27(9)	1.6(1)
Occ.	1.0	1.0	1.0	1.0
M2 in $32e$ (x, x, x)	32Ni	31Al + 1Ni	32Al	32Al
x	0.2136(1)	0.2077(2)	0.2079(2)	0.2087(1)
$B_{eq}.(B_{iso})\ 10^2$ (nm^2)	2.05(1)	1.46(9)	2.1(2)	1.2(1)
Occ.	1.0	1.0	1.0	1.0
M3 in $16d$ (1/2, 1/2, 1/2)	—	16N	16N	16O
$B_{eq}.(B_{iso})\ 10^2$ (nm^2)		1.1(3)	2.6(5)	1.8(1)
Occ.		1.0	1.0	0.75
M4 in $16c$ (0, 0, 0)	16Ti	15Ni + 1Al	16Ni	16Ni
$B_{eq}.(B_{iso})\ 10^2$ (nm^2)	1.9(2)	1.31(8)	2.7(2)	1.7(1)
Occ.	1.0	1.0	1.0	1.0
Distances (nm) within the first nearest neighbor co-ordination; standard deviations are < 0.001 nm				
M1 2M3	—	0.2125	0.2126	0.2137
2M2	0.2579	0.2699	0.2695	0.2688
2M2	0.2899	0.2948	0.2946	0.2925
2M4	0.2908	0.2943	0.2942	0.2927
4M1	0.2951	0.2988	0.2990	0.3014
4M1	0.2988	0.3023	0.3023	0.3028
M2 3M4	0.2468	0.2457	0.2458	0.2466
3M1	0.2579	0.2699	0.2695	0.2688
3M2	0.2814	0.2658	0.2665	0.2694
3M1	0.2899	0.2948	0.2946	0.2925
3M3	—	0.3392	0.3389	0.3381
M3 6M1	—	0.2125	0.2126	0.2137
M4 6M2	0.2468	0.2457	0.2458	0.2466
6M1	0.2908	0.2943	0.2942	0.2927

Note. Space group $Fd\bar{3}m\text{-}O_h^7$ (No. 227); origin at center, $Z = 2$. Ti_2Ni type. Standard deviations in parentheses.

$2\theta = 34.1°$, (222) at $2\theta = 27.1°$ and (622) at $2\theta = 53.4°$. The atom arrangement in $Ti_3NiAl_2O_{1-x}$, being significantly different from that in Ti_2Ni or Ti_4Ni_2O, reveals a larger unit cell dimension when compared to Ti_2Ni or Ti_4Ni_2O (see for instance Fig. 4). Although our lattice parameter for Ti_3NiAl_2O is slightly lower than that for the reported x phase, the dependency on atom sites in combination with the characteristic intensity relations would suggest that the x phase reported by Umemoto and co-workers (8–10) may well be labeled as $Ti_3NiAl_2O_{1-x}$ rather than a ternary compound with $(Ti,Al)_2(Ni,Al)$ stoichiometry.

CONCLUSION

The phase equilibria in the Ti–Ni–Al–N and Ti–Ni–Al–O systems were determined from bulk alloys. Two quaternary compounds Ti_3NiAl_2N and $Ti_3NiAl_2O_{1-x}$ with the filled Ti_2Ni type were found to exist. The characteristic

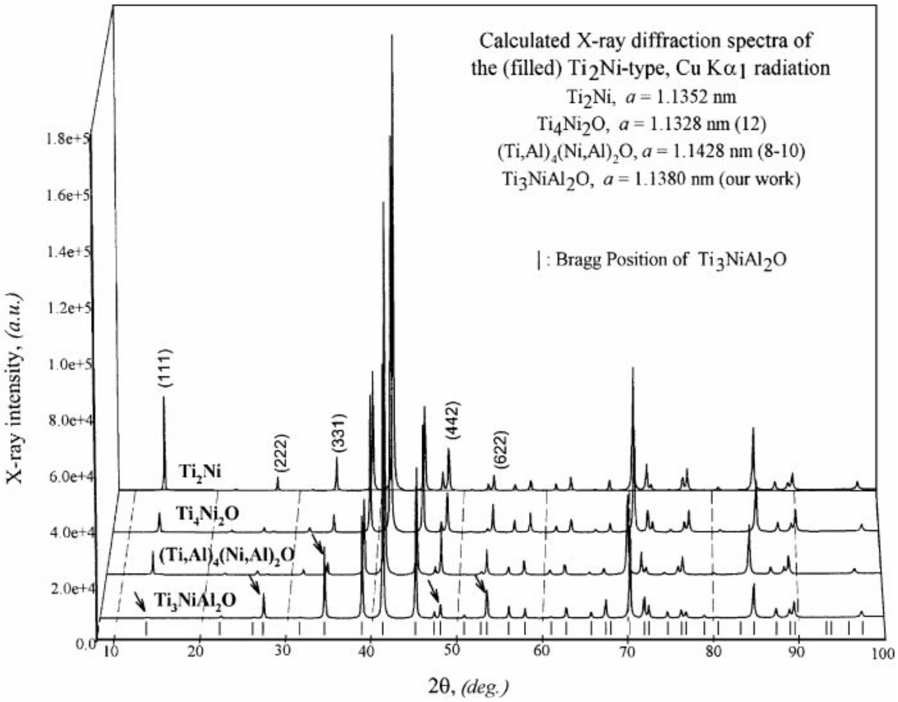

FIG. 4. Comparison of calculated X-ray spectra of Ti_2Ni-type phases: Ti_2Ni, Ti_4Ni_2O, $(Ti,Al)_4(Ni,Al)_2O$, and Ti_3NiAl_2O.

differences of X-ray spectra among the various compounds with Ti_2Ni-type parent structure, Ti_2Ni, Ti_4Ni_2O, and $Ti_3Ni\ Al_2O$, were analyzed. Rietveld refinements were presented for Ti_3NiAl_2N and $Ti_3NiAl_2O_{1-x}$.

ACKNOWLEDGMENTS

Financial support of this research by the Austrian Ministry of Science under Grants GZ 49.885/2-II/4/93 and GZ 140.601 is gratefully acknowledged. Thanks are furthermore due to the Austrian/Chinese technical scientific exchange programme (Project V. A. 15) as well as to Dr. H. Schmidt for his assistance with EMPA.

REFERENCES

1. P. Nash and W. W. Liang, *Metall. Trans. A*. **16,** 319 (1985).
2. B. Huneau, P. Rogl, K. Zeng, R. Schmid-Fetzer, M. Bohn, and J. Bauer, *Intermetallics* **7,** 1337 (1999).
3. J. Rodriguez-Carvajal, *in* "Abstracts of the Satellite Meeting on Powder Diffraction of the XV Congress of the International Union of Crystallography," p. 127. Talence, France, 1990.
4. J. L. Pouchou and F. Pichoir, *J. Microsc. Spectrosc. Electron.* **10,** 279 (1985).
5. E. Reiffenstein, H. Nowotny, and F. Benesovsky, *Monatsh. Chem.* **96,** 1543 (1965).
6. P. Rogl and H. Nowotny, *Monatsh. Chem.* **108,** 1167 (1977).
7. S. Sridharan, H. Nowotny, and S. F. Wayne, *Monatsh. Chem.* **114,** 127 (1983).
8. M. Umemoto, T. Norimatsu, and T. Itsukaichi, *J. Jpn. Inst. Metals* **57,** 1209 (1993).
9. T. Itsukaichi, M. Umemoto, and J. G. Cabanas-Moreno, *Scripta Metall. Mater.* **29,** 583 (1993).
10. J. G. Cabanas-Moreno, T. Itsukaichi, and M. Umemoto, *Mater. Sci. Engng. A* **181/182,** 1202 (1994).
11. J. J. Ding, P. Rogl, B. Chevalier, and J. Etourneau, *Intermetallics*, in press.
12. M. H. Mueller and H. W. Knott, *Trans. Metall. Soc. AIME* **227,** 674 (1963).